EFFECTS OF MODE OF SECONDARY AIR INJECTION ON THE GAS AND SOLIDS VELOCITY PROFILES IN A CIRCULATING FLUIDIZED BED RISER

Levent E. ERSOY, Murat KOKSAL, Feridun HAMDULLAHPUR

Department of Mechanical Engineering, Dalhousie University
Halifax, Nova Scotia, B3J 2X4, Canada

ABSTRACT - The effects of the emerging patterns of the secondary air (SA) jets on the particle velocity profiles in the lower sections of a CFB riser were studied experimentally. The problem of jet emerging in a single-phase flow was also simulated for the radial and tangential SA injection cases using a commercial software, Fluent V4.4. The results showed that the initial orientation of the lateral momentum imposed by the strong SA jets caused a solid body obstruction over part of the riser cross section. Further, it completely altered the mixing pattern of secondary air with primary air.

INTRODUCTION

Air staging is an effective way of controlling the NO_x formation in circulating fluidized bed (CFB) combustion of highly volatile fossil fuels (Brereton, 1997; Leckner, 1998). The secondary, or sometimes tertiary air, is also utilized to control the bed temperature which has a direct influence on the emission characteristics of the CFB combustors (Hippinen *et al*. 1993). A number of investigators worked on the effects of a laterally injected stream on the gas and solid patterns in a riser (Marzocchella and Arena, 1996a,b; Ersoy *et al*. 1997). These studies showed that the secondary to primary air flow ratio (SAR), the height of injection and the mode of injection can be considered as important design parameters of SA injection. Different types of SA injection devices result in different gas and solid velocity, mass flux and mixing patterns (Marzocchella and Arena, 1996a,b; Ersoy, 1998).

This paper reports the experimental findings on the effects of mode of injection (radial and tangential) on the particle axial velocity field and the results of the single-phase, three-dimensional, CFD simulations in the riser.

EXPERIMENTAL SETUP

A schematic diagram of the experimental set-up is shown in Figure 1. The riser (7.6 m high, 0.23 m ID) and the modular SA injection unit are made of Plexiglas and steel, respectively. The injection unit has two adjustable injection nozzles. The alignment of the nozzle pair determines the mode (orientation) of air injection. The straight sections were made of 0.0397 m ID steel pipe. The pipes were long enough to ensure fully developed airflow before the nozzle tip. The air jets were arranged to penetrate into the riser from only two locations around the periphery to ensure closer operational similarity with commercial boilers. The solid particles used in the experiments were FCC catalyst, with a mean particle diameter of 60 μm and a particle density of 1500 kg/m^3. A fixed external solids circulation rate (G_s = 18 kg/m^{2}s) was used in all experiments. The total gas flow (the sum of the primary and secondary air flows) was also kept constant with a superficial gas velocity of U_0 = 3 m/s.

The secondary air was injected into the riser through two horizontally symmetric ports located at a height of 1.2 m above the distributor plate. An optical probe (Vector VSI-2000) composed of two 1 mm diameter bundles of optical fiber spaced 4 mm apart, was used for particle velocity measurements. For the radial case, the axial velocity profiles were measured along a plane perpendicular to the SA nozzles horizontal axis; whereas they were measured along a plane parallel to the SA nozzles horizontal axis for the tangential case. A detailed explanation of the experimental set up and measurement system can be seen elsewhere (Ersoy *et al*. 1997; Ersoy, 1998).

THREE-DIMENSIONAL, SINGLE-PHASE CFD SIMULATIONS

To investigate the effects of the SA jets and their penetration patterns into the riser for radial and tangential injections, a three-dimensional flow model was formulated and subsequently, single-phase, CFD simulations were carried out using a commercial software, Fluent V4.4. Two different turbulence closure models were used for each injection mode case. The three-dimensional, incompressible, Navier-Stokes equations were closed using the standard k-ε turbulence model for the radial injection case, and the RNG k-ε model for the tangential injection case (Launder and Spalding, 1974; Yakhot and Orszag, 1986). The RNG k-ε model considers the variation of the effective viscosity with eddy size and local vorticity, thus, it is more suitable for flows with high strain rates and curvilinear coordinates such as swirling flows. The computational grids constructed represent the experimental set-up of this work. The three-dimensional grid constructed for tangential injection simulations consisted of 68 479 cells (47X47X31), covering a 3.5-m portion of the riser, starting from 0.5 m below the SA injection plane. The grid for radial SA injection was composed of 38 326 cells (41X26X36) and covered only one half of the riser diameter since the radial injection problem was considered as symmetric about a vertical plane in the mid section of the SA injection port. The simulations were carried out for U_0 = 5 m/s and SAR = 0.5. Hence, the primary and secondary gas inlet velocities were set to be 3.37 m/s and 27.85 m/s, respectively.

RESULTS AND DISCUSSIONS

Figures 2a,b,c,d compare the radial variations of the axial component of particle velocity at different heights in the riser for radial and tangential SA injection and non-SA operation at a constant total air flow rate. As can be seen in Figures 2a and 2b, where the velocity test sections are below the SA injection port, the axial component of the particle velocity is lower in the primary region when the fluidization air is staged due to the reduced air flow rate in the primary region, regardless of the mode of injection. At lower parts of the riser (68 cm below SA injection), the particle velocity profiles become insensitive to the mode of SA injection (Figure 2a). The effect of mode of SA injection on the particle velocity field becomes more pronounced at locations closer to the SA injection port. Figure 2b shows that at 17 cm below the SA injection port, radial injection results in a flatter velocity profile with a lower magnitude in the core region when compared to tangential SA injection. On the other hand, tangential injection of SA imposes higher velocity values in the core region with a smaller core radius. It is also interesting to note that, despite the lowered primary superficial gas velocity, particles just below the SA port gain considerable acceleration, reaching values very close to the velocity of non-SA operation near the wall region ($r/r_0 > 0.8$). The increase in the particle velocity just below the SA injection port can be attributed to the size effects of secondary air jets, which result in contraction of the flow area. Depending on the SAR, the jets may occupy a portion of the riser cross section assuming a form similar to a three dimensional solid body. This obstruction forces the upcoming flow to go around the “blockage” and flow through the contracted area. For the tangential injection case, the area contraction phenomenon may be considered analogous to the flow in a converging diverging nozzle; whereas in the radial injection case, extending over the diameter of the riser column, SA jets may divide the circular cross section into two regions depending on their momentum.

Figure 2c shows the axial particle velocity profile at the third level (6 cm above the SA injection plane). It should be noted that, unlike the other test sections in the riser, the mean particle velocity, even in the close vicinity of the wall was found to be upwards regardless of the mode of injection. This behavior can be accepted as a proof that the presence of secondary air jets not only blocks a portion of the up-rising suspension from the primary region, but also blocks the down-coming suspension in the annulus. This may also prevent the gas backmixing which is mainly due to the solids downflow near the wall. Although the particle velocity in the wall region was measured as mostly upwards just above the SA injection plane, measurements revealed the existence of an annulus region at 62-cm above the SA injection plane. Figure 2d shows that the annulus region in this section is thinner than it is for the non-SA operation. In the core annulus interface, radial SA injection results in wider core region, while the tangential injection results in a flatter velocity profile in the core region and a thicker annulus.

The single-phase numerical simulations revealed very useful information on the mixing patterns of the secondary and primary air streams. Figure 3 shows the effects of tangential and radial jets on the axial velocity distribution at the middle vertical slice of the riser. The presence of a downward velocity in the wall region reveals that the primary air is forced to accelerate and proceed through the core section whose boundary is determined by the momentum of the SA jets. On the other

hand, the radial SA jets results in a major distortion in the flow of the primary air. It can be seen that, for SAR = 0.5, the SA jet is strong enough to be effective over the whole column diameter, and the upcoming suspension is separated into two streams advancing through the sides of the riser.

The local non-uniformity associated with the mode of injection can be best seen at the cross sectional plane of SA injection (Figure 4). The contours of total pressure show that the SA jets are effective over the whole radius for SAR= 0.5, for radial injection. The local low-pressure regions, created outside the boundary of SA jets, are the regions of high axial velocity which extend axially both upstream and downstream of the SA injection plane. In the tangential injection case, the annulus is thicker in the close vicinity of the SA jet inlets, which considerably reduces the upward flow area.

Figure 5 shows the contours of effective viscosity along the center vertical plane of the riser. The addition of secondary air forms a high kinetic energy region along the path of the SA jets. It is interesting to see that the remarkable difference in the effective viscosity of the PA and SA streams does not diminish immediately just above the injection plane, but prevails over a long section of the riser. In the tangential SA injection case, the SA jets diffuse gradually from the wall region inwards and result in a more homogenous upper bed. This axial non-uniformity in the viscosity profile for radial SA injection suggests poor mixing compared to its tangential counterpart. The mixing in terms of uniform turbulent energy is completed in a shorter axial distance if SA is injected tangentially.

CONCLUSIONS

The results of particle axial velocity measurements and their variations in the radial direction are presented for tangential and radial SA injection cases. Comparisons with that of non-SA operation reveal that the emerging patterns of SA jets may alter the particle velocity field by creating a local hydrodynamic blockage. The tangential SA injection forces the upcoming suspension to proceed through the core region, resulting in more parabolic velocity profiles in the radial direction, whereas, the radial SA injection flattens the profiles while causing the upcoming suspension to proceed from the sides of the riser, away from the SA jets. A three-dimensional, single-phase, CFD study was also performed to understand the jet emerging and gas-gas mixing patterns imposed by different SA injection modes. Results show that the lateral momentum imposed by the horizontal SA jets creates local high and low pressure regions in the vicinity of the SA injection plane. Therefore, injection of SA not only creates a local hydrodynamic blockage, but also results in completely different gas mixing patterns throughout the riser depending on the mode of SA injection. The authors are also aware of the fact that, although the results of the single-phase CFD simulations provided useful information about the gas phase hydrodynamics with SA injection, its extrapolation to the actual case with the presence of the particles should be done with caution. Therefore, the current research is directed to further investigate the effects of SA injection on gas mixing by using gas tracer technique and perform three-dimensional, two-phase, Eulerian-Eulerian (two-fluid) CFD simulations.

NOTATION

PA	Primary air
R	Radial Injection
r/r_0	Non-dimensional radius
SA	Secondary air
SAR	Secondary to primary air flow ratio
T	Tangential Injection
U_o	Superficial gas velocity, m/s
z	vertical distance from the distributor, m

ACKNOWLEDGEMENTS

Fluent 4.4 used in the simulations is provided by Fluent. Inc under educational license agreement.

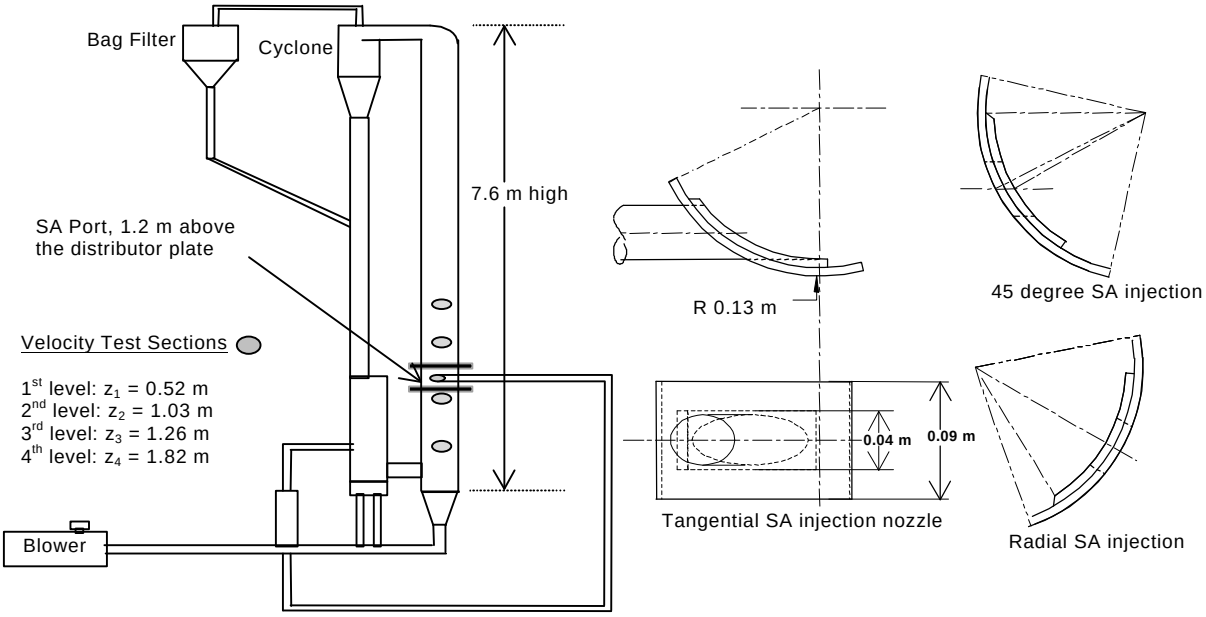

Figure 1. Experimental set-up and various secondary air injection nozzles

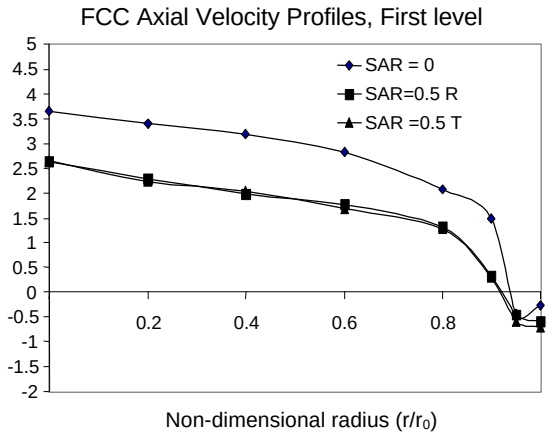

(a) 68 cm below SA injection

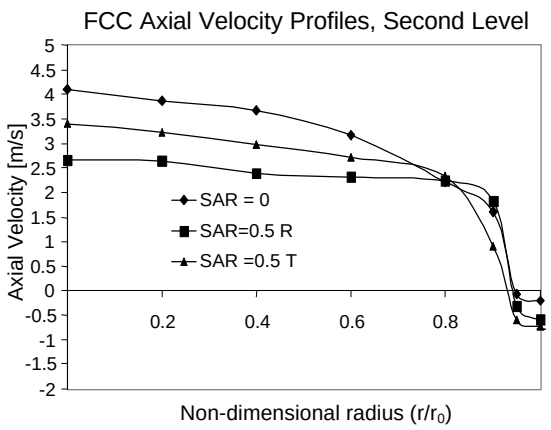

(b) 17 cm below SA injection

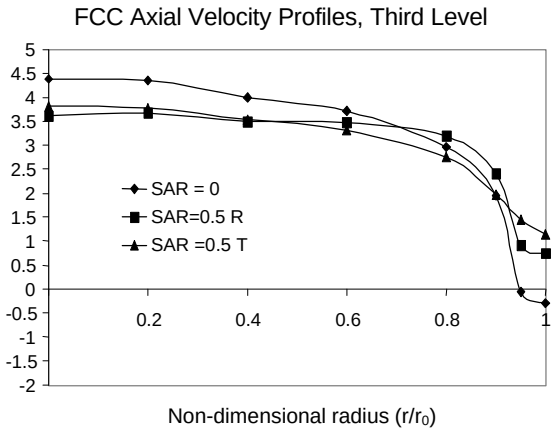

(c) 6 cm above SA injection

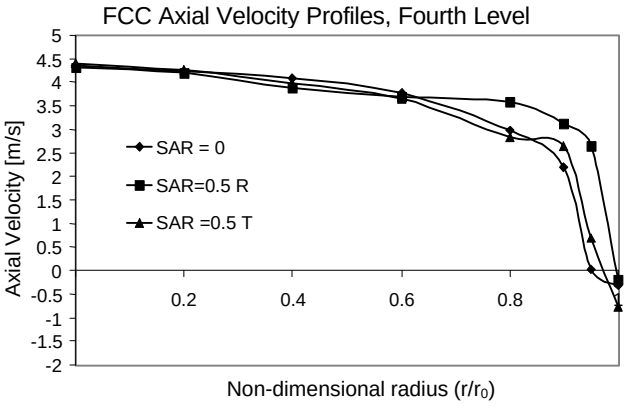

(d) 62 cm above SA injection

Figure 2. Effect of mode of SA injection on radial variation of particle axial velocity.

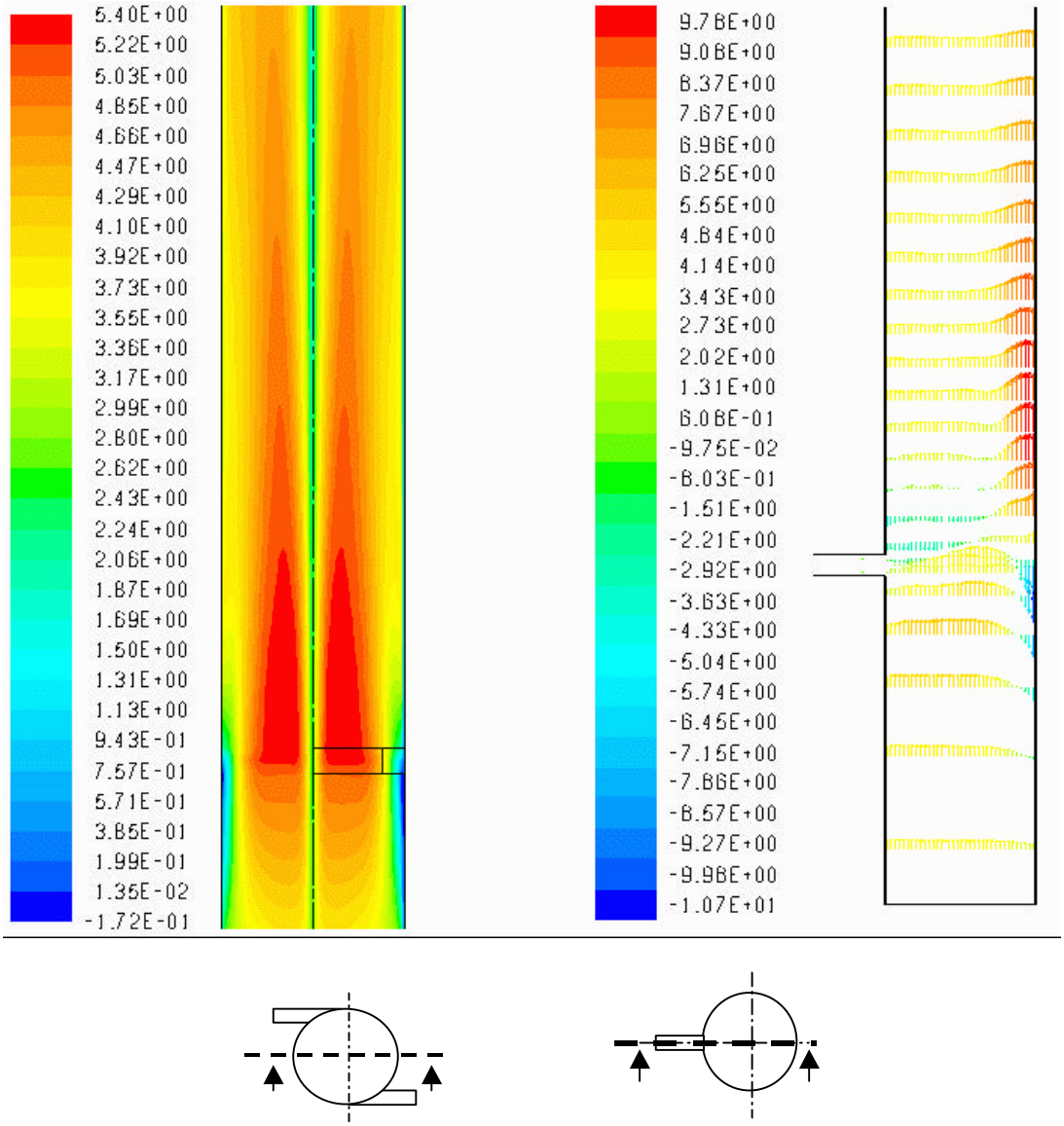

Figure 3. Effect of SA injection on the gas axial velocity field for tangential and radial SA orientations (Axial particle velocity is in m/s)

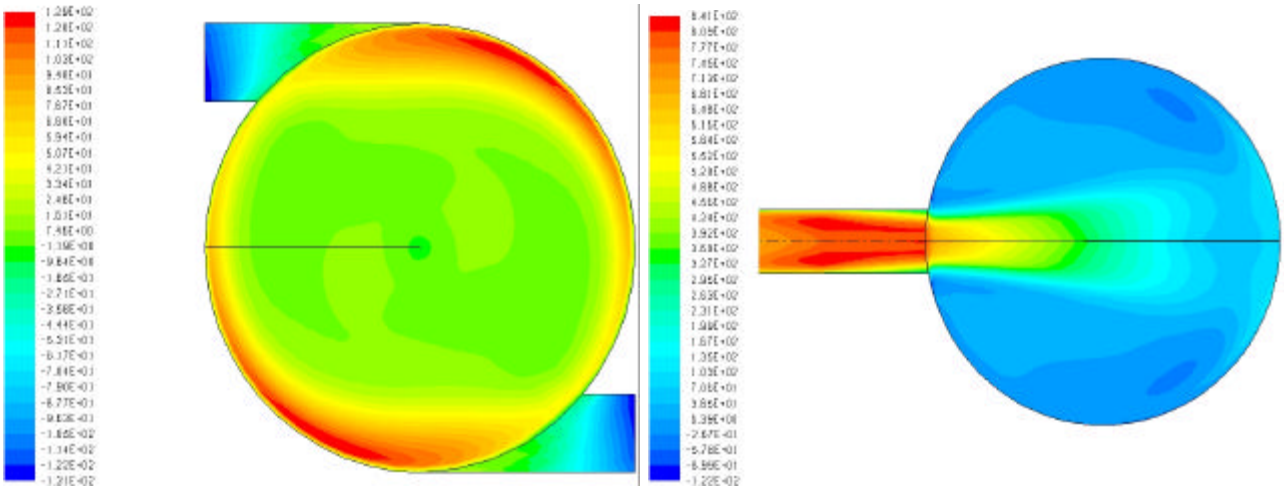

Figure 4. Effect of jet emerging patterns on the total pressure field at the horizontal plane of SA injection (Total pressure is in Pa)

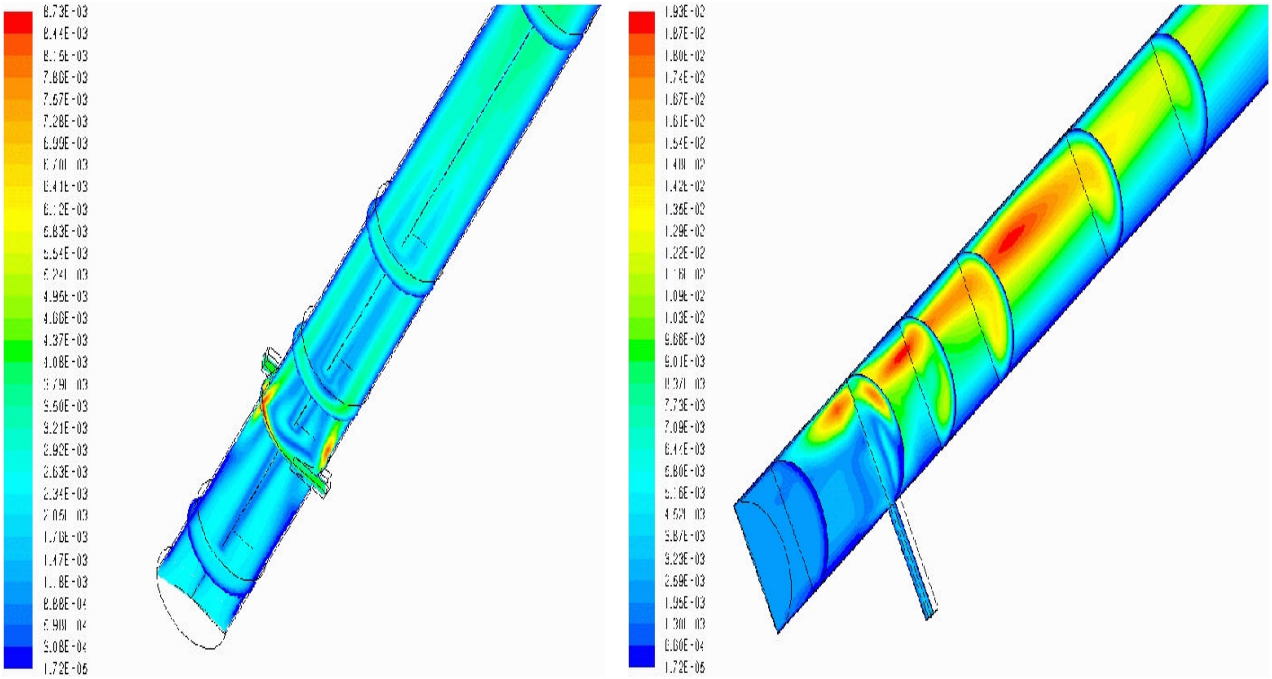

Figure 5. Effect of mode of SA injection on the effective viscosity distribution along the riser axis (center vertical plane, effective viscosity is in Pa.sec).

REFERENCES

Brereton, C., “Combustion Performance” in Circulating Fluidized Beds, eds., Grace, J.R., Avidan, A.A., Knowlton, T.M., chp. 10, pp. 369-416, Chapman & Hall, London, 1997.

Ersoy, L. E., Militzer, J., Hamdullahpur, F., “Effect of Secondary Air Injection On the Hydrodynamics of Circulating Fluidized Beds”, Proceedings of 14th Int. Conf. On Fluidized Bed Combustion, vol. 2, pp.1247, ASME, Vancouver, 1997.

Ersoy, L.E., "Effect of Secondary Air Injection on the Hydrodynamics of CFBs", PhD Thesis, Dalhousie University, 1998.

Hippinen, I., Lu, Y., Jahkola, A. The Effect of Combustion Air Staging on Combustion Performance and Emissions in PFBC, Proceedings of 12th Int. Conf. on Fluidized Bed Combustion, ed., Rubow, L.N., pp. 117-121. ASME, San Diego, CA., 1993.

Launder, B.E., Spalding, D.B., “The Numerical Computation of Turbulent Flows”, Computer Methods in Applied Mechanics and Engineering, v. 3, pp. 269-289, 1974.

Leckner, B., “Fluidized Bed Combustion: Mixing and Pollutant Limitation”, Progress in Energy and Combustion Science, vol. 24, pp. 31-61, 1998.

Marzocchella, A., Arena, U., “ Hydrodynamics of a Circulating Fluidized Bed Operated with Different Secondary Air Injection Devices”, Powder Technology, vol. 87, pp. 185-191, 1996a.

Marzocchella, A., Arena, U., “Mixing of a Lateral Gas-Stream in a Two-dimensional Riser of a Circulating Fluidized Bed ”, The Canadian Journal of Chemical Engineering, vol. 74, pp. 195-202, 1996b.

Yakhot, V., Orszag, S.A., “Renormalization Group Analysis of Turbulence, 1. Basic Theory”, Journal of Scientific Computing, v. 1(1), pp. 3-51, 1986.